https://doi.org/10.15407/ujpe63.11.994

I.YE. MATYASH, I.A. MINAILOVA, O.M. MISCHUK, B.K. SERDEGA

V.E. Lashkaryov Institute of Semiconductor Physics, Nat. Acad. of Sci. of Ukraine
(41, Nauky Ave., Kyiv 03028, Ukraine; e-mail: irinaminailova125@gmail.com)

COMPONENT ANALYSIS OF RADIATION-INDUCED THERMOELASTICITY USING MODULATION POLARIMETRY

A radiation field of an external or internal origin creates a non-uniform temperature gradient in a glass specimen. In this case, there appears a heat flux in the specimen, which generates mechanical stresses and induces an optical anisotropy in the form of birefringence. In this work, using the optical-polarization method, the birefringence magnitude is measured as the phase difference between the orthogonal components of the linearly polarized probing radiation. The capability of the method is enhanced by modulating the radiation polarization, which provided a reliable registration of stresses in the specimen at a temperature drop of about 0.1 K. The stress kinetics with a complicated behavior and ambiguous by sign is detected at the observation point within the temperature establishment time interval. Its modeling in terms of exponential functions made it possible to decompose the measurement results into components associated with the radiative, conductive, and convective heat transfer mechanisms, as well as determine their relaxation parameters. The measurement data can be of practical use while determining such technically important material characteristics as the thermal diffusion and heat transfer coefficients.

K e y w o r d s: thermoelasticity, modulation polarimetry, radiative, conductive and convective heat transfer mechanisms.

1. Introduction

The thermal expansion of a homogeneous solid is known to be confined by the non-uniformity of a temperature gradient under heat flux conditions [1]. In this case, the non-uniform character of the temperature-induced expansion of a substance becomes responsible for the thermal stresses that arise in it. The study of those phenomena is a matter of interest in elastostatics and elastokinetics. These two domains of solid-state physics describe a relationship between the deformation-induced elastic fields in the substance and the temperature field parameters, the latter, in turn, being related to the deformation energy [2]. This area of mechanics is based on the synthesis of the classical theory of elasticity and the theory of thermal conductivity. Having obtained a significant impetus within last decades, this science became the source of a large number of publications. Therefore, for the results of researches in this area to be convenient for understanding, it is expedient to represent them in a structured form.

For instance, heat fluxes can be excited using a dozen of methods [3]: contact, radiation (infrared and corpuscular), laser (pulsed and stationary), sound, mechanical shock, friction, and so forth. This list can be appended by about the same number of physical effects, as well as experimental methods of their registration. Conditionally, those methods are divided into two related groups associated with the factors

that are the most commonly used to study deformations in solids. This is a variety of methods for the thermal generation of stresses and the variants of the optical-polarization registration of the birefringence [4–6].

In this work, we deal with the same two physical entities: the thermo-elastic effect and the optical method of its registration, each of them possessing its own element of a certain novelty. First of all, this statement concerns the examined specimen that loses its internal energy through thermal radiation. Such a state of the researched object is associated with a certain spatial inhomogeneity of the radiation field, where the specimen is located, and, as a result, with a negative radiation balance inside it. Hence, it follows that, in the case of experiments under room conditions, the decrease of the temperature at the specimen ends may be equal to a few degrees below the room value. In such a case, the measurement of small mechanical stresses requires the application of unique methods and facilities that could reliably register all peculiarities in the process of establishment of elastokinetic and elastodynamic states.

An example of such methods is modulation polarimetry (MP), which is classified to spectrometry [7]. It includes some elements of differential spectroscopy [8] and, therefore, is characterized by the inherited analytical and high detection capabilities. In work [9], we showed that MP can be used to register thermal stresses, even if all mechanical and optical coefficients that are involved in the stress generation are almost temperature-independent. Therefore, the aim of this work is to continue and further develop researches started in work [9] and dealing with the peculiarities of radiation thermoelasticity in the case where the stresses are induced by external thermal radiation.

However, as was marked in work [10], the radiation cooling of a solid is also accompanied by the appearance of internal stresses. A detailed study of the latter has, first of all, an academic interest owing to the asymmetry of the conditions for external and internal radiations. We do not know about publications in the domain of solid state physics that are devoted to the radiation cooling, except for work [11], in which the impulse method was applied to register a negative radiation balance in a semiconductor crystal as a result of the free electron removal from its volume.

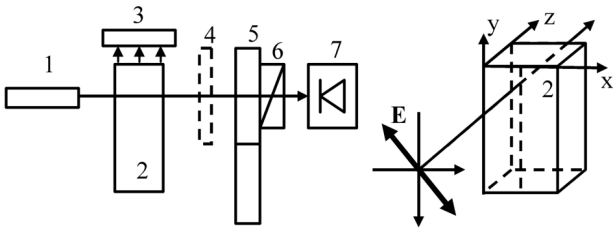

Fig. 1. Schematic diagram of the experimental registration of thermoelasticity induced by the radiation cooling and heating: He-Ne laser (*1*), specimen (*2*), electrothermal element (*3*), compensating phase plate (*4*), photoluminescence polarization modulator (*5*), polarizer (*6*), and Si photodetector (*7*)

However, more important are practical circumstances associated with the radiation cooling of materials that are fabricated or thermally treated at temperatures up to 1000 [12] and 2000 K [13]. The real-time registration of processes running under such conditions becomes problematic, if impossible at all. In this case, there is a ground to hope for that their modeling at lower temperatures, due to the detection capability of MP, which is sufficient for this purpose, will make it possible to obtain results that can be extrapolated to the indicated conditions.

Additionally, it is worth noting that the radiation cooling, which is controllable in our case, can be used to model such processes as the night cooling of the Earth surface [14], buildings [15], and thermal energy accumulators [16]. We would also like to dissociate ourselves from a large number works like [17, 18], in which the term "radiation cooling" is used to denote the technology of cold production on the basis of materials with martensitic transformation properties.

2. Experimental Technique

The thermoelastic properties of solid specimens were studied by measuring the spatial distributions of mechanical stresses induced in them at the radiation cooling, as well as their temporal evolution. The measurements were carried out on a polarimetric installation (Fig. 1), whose main component is photovoltaic polarization modulator *5*. By appropriately arranging the functional elements (the modulator and linear polarizer *6* were arranged behind the specimen), the installation was configured to register the linear birefringence, which was described in detail in work [9]. Therefore, here, we only describe the differences.

A rectangular parallelepiped specimen *2* with the dimensions $l_x \times l_y \times l_z = 2 \times 3 \times 2$ cm^3 was cut out from glass TF-1. This choice was stimulated by the optical homogeneity of this material, as well as by the correspondence between the characteristic times of heat transfer processes and the registration equipment. All specimen surfaces were subjected to a standard treatment (grinding, polishing) to minimize structural defects of them and resulting residual stresses. The specimen was irradiated with the help of an electrothermal (Peltier) element *3*. Its size slightly exceeded the size of the end xz-surface of the specimen, which provided conditions for the field uniformity in the near-surface region.

The specimen was cooled down from 295 K (room temperature) to 292 K. The measurements were carried out under environmental conditions at atmospheric pressure. Therefore, the specimen was shielded from fluctuations of convective fluxes in order to reduce the instability of a measured signal. The Peltier element was cooled/heated at a certain distance from the specimen until it reached a stationary regime. Its effect (cooling or heating) was "switched on" by arranging this element above the specimen with the help of a rotator.

From the optical diagram depicted in Fig. 1, it follows that the direction of the heat flux in the specimen determines the orientation of the Fresnel ellipsoid (the indicatrix of refractive indices) in such a way that the axes of the latter become oriented along the x- and y-axes of the specimen. In this case, radiation (the wavelength $\lambda = 650$ nm, the diameter of the normal cross-section of the laser beam (*1*) equals 0.1 mm) must be so linearly polarized that the azimuth of the electric field vector **E** of the wave with respect to the specimen axes should be equal to 45°. In this geometry, the equality condition $E_x = E_y$ for two components of the wave field is optimal from the viewpoint of the effective transformation of radiation into a circularly polarized one at its propagation in the anisotropic specimen. This conclusion follows from the properties of polarization optics [19].

Namely, the intensity of the circularly polarized component is determined by the expression $I_V = E_x E_y \sin(\Delta\phi)$, where $\Delta\phi$ is the phase difference between the orthogonal linear components. It equals $\Delta\phi = 2\pi(d/\lambda)\Delta n$, where d is the specimen thickness in the radiation propagation direction, and $\Delta n = n_x - n_y$. Since the wavelength λ of the probing radiation and the specimen thickness d in the direction of radiation propagation are known, the intensity I_V corresponds to the magnitude and sign of the optical anisotropy Δn. In the case $\Delta\phi \ll 1$, which is valid for our measurements, and small deformations (within the limits of Hooke's law), the optical anisotropy is a measure of the mechanical stress: $\Delta\phi = C\sigma$. The stress-optical coefficient (the phase incursion per mechanical stress unit [20]) is determined by an additional anisotropy measurement, when the specimen is deformed by an external controlled force. Thus, the magnitude and sign of the circular radiation component emitted from the specimen contain information about the magnitude and sign of internal mechanical stresses arising owing to thermoelasticity.

Thermal stresses as the magnitude of the circular component normalized by the stress-optical coefficient, $I_V \propto \Delta\phi/C$, were registered in the form of their time dependences at fixed positions of a probing beam (the y-coordinates). The signal from photodetector *7* was measured using a lock-in nanovoltmeter at a modulation frequency of 50 kHz. The selective registration of the signal and a rather high frequency of the latter allowed us to reliably register small mechanical stresses. At a deformation of 10^2 Pa, the signal-to-noise ratio was equal to 10. When measuring at a fixed coordinate, the residual mechanical stresses were compensated by phase plate *4*, which allowed measurements reckoned from the zero reference value to be carried out. The positive sign of the signal was established using the phase of the reference signal from a synchronous amplifier or by changing the azimuth of the wave electric field by 90°. The positive sign corresponded to the squeezing of the specimen along its y-coordinate.

3. Measurement Results and Their Discussion

We would like to emphasize that, when studying the radiation thermoelasticity of a glass specimen irradiated with thermal radiation emitted by a black body, we have registered the radiation cooling [9]. This phenomenon, which accompanies the cyclic heating-cooling process, manifests itself as the relaxation of the specimen to an equilibrium state, when the radiation heating had been terminated. In the present work, the matter of concern is the radiation cooling of a solid and the corresponding internal stresses and

birefringence. The inevitability of the radiation cooling is dictated, first of all, by the spectral difference between the absorption (radiation) coefficients of the black body and the specimen. Furthermore, it is not ruled out that the smallest changes in the amplitude ratio between the heat transfer components will result in significant modifications of general characteristics.

Those speculations formed a basis of an experiment, whose result is shown in Fig. 2. Here, the magnitude of the mechanical stress at one of the specimen coordinates was obtained by continuously measuring the birefringence in four cycles under varied conditions. The test point with the coordinate $y = 7$ mm was chosen as producing the most informative form of the curve. Two cycles, the first and the third one, included the external coercive actions on the specimen, namely, the radiation cooling and heating, respectively. In the other two cycles, the second and fourth ones, inverse processes took place: the relaxation of the temperature and stress gradients in the specimen to the equilibrium state under the natural heating and cooling, respectively. In all four cases, the time of the stationary state establishment was determined from the condition that the magnitude of the corresponding influence had to be constant.

One can see that the extrema have opposite signs in each pair of heating-cooling characteristics, which can be associated with changes in the heat flow direction and, therefore, the signs of the radiation field gradients. The actual reason consists in that, according to the Poisson law, the stress σ is not generated by the gradient of the potential function $\phi(y)$ (the temperature in this case), but by its curvature at the test point, $\operatorname{div}\phi \propto \pm\sigma$. In a real experiment, the sign of the birefringence $\Delta n = n_x - n_y$ changes due to the change of the optical indicatrix (Fresnel ellipsoid) azimuth by 90° with respect to the specimen coordinates at a fixed azimuth of the wave E-field (Fig. 1).

Note also that the curves obtained for the direct and inverse cooling-heating cycles are consistent with one another, which can be verified by applying the translational symmetry. However, a more important fact is that each of four parts in the general characteristic contains the same features like fast and slow relaxation sections separated by two extrema. Whence it is not difficult to make a conclusion that each of them consists of three sections that are different not only by amplitudes, but also by trends.

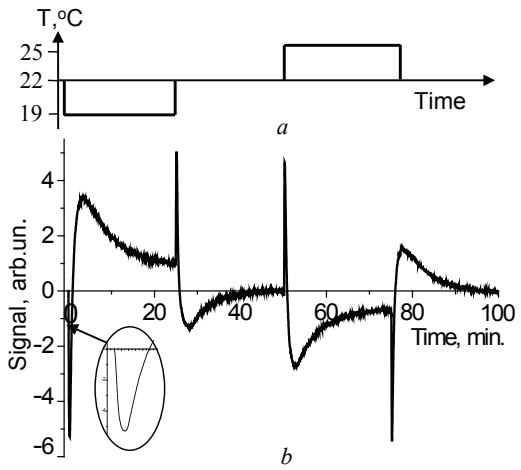

Fig. 2. Kinetics of the specimen surface temperature under the radiation cooling and heating (a). Kinetics of the mechanical stress induced in the specimen by, sequentially, the radiation cooling (0–25 min), environmental heating (25–50 min), radiation heating (50–75 min), and environmental cooling (75–100 min) (b)

Let us analyze the first plot section. The corresponding results may be appropriate to other three sections. The analysis is based on two fundamental factors. which were discussed above. One of them is a high detectable capability of MP with respect to low anisotropy values and their reliable registration at insignificant temperature drops across the specimen. The second factor follows from the first one. Under the described conditions, the parameters that are responsible for the thermal stress generation (Young's modulus, heat transfer and linear expansion coefficients) or participate in its registration (refractive index, stress-optical coefficient, Poisson's ratio) are almost temperature-independent. In this case, one may hope for that, owing to the linear character of the equations describing the emergence of thermal stresses and their relaxation, their solutions are exponential functions.

In what follows, we will use the evident fact that two of three functions participating in the formation of the first section of the characteristics in Fig. 2 reached the saturation within the time intervals $t \approx$ $\approx$ 0.65 min and $t \approx 6$ min. Therefore, the longest dispersion component of the complex function has grounds to be elementary. Really, on the log scale, this is a straight line spanning a few orders of magnitude. Its slope is determined by the characteristic

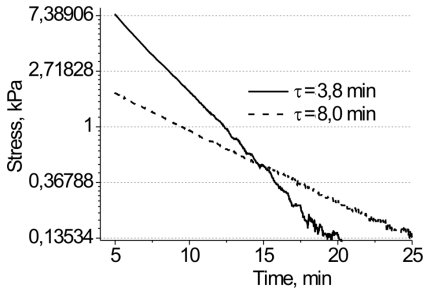

Fig. 3. Determination of the characteristic time for the establishment of a convection-induced stress at a shielding from convection fluxes (dashed curve) and under forced-convection conditions (solid curve)

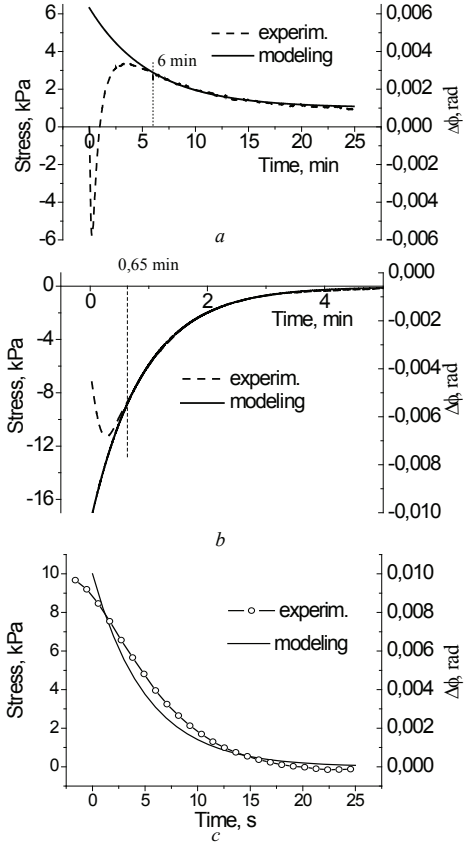

Fig. 4. Mechanical stress components and their approximations by exponential functions: convective component, $\sigma_{conv} = 5.3\exp(-t/\tau)+1.02$, $\tau = 5.75$ min (a); conductive component, $\sigma_{\rm cond} = 16.3\exp(-t/\tau)$, $\tau = 1.01$ min (b); and radiative component, $\sigma_{\rm rad} = 10.0\exp(-t/\tau)$, $\tau = 4.1$ s (c). The values of mechanical stress components (left axis) were obtained by normalizing a change $\Delta\phi$ of the phase difference between linear orthogonal components (right axis) determined from an additional measurement

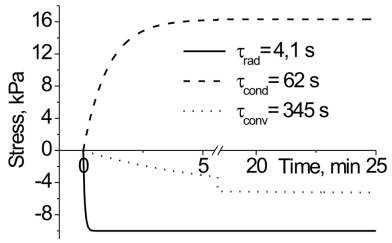

Fig. 5. Kinetics of thermally induced stress components generated by three heat transfer components

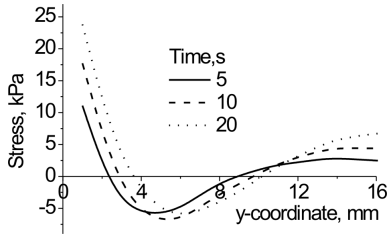

Fig. 6. Time evolution of the total stress profle along the y-coordinate of the specimen

relaxation time. The result of this procedure is exhibited in Fig. 3, which illustrates the relaxation rate for two variants: the shielded and forced convections in the specimen environment. An appreciable response of the cooling process to changes in the environmental conditions enables us to connect this section with the convective component of heat transfer. On this basis, we may take a model exponential function and ascribe such an amplitude of the steady state to it that provides the best agreement with experiment (Fig. 4, a).

The obtained model function enables the section of the curve located within the interval $0 < t < 6$ min and consisting of two components to be decomposed further. The decomposition is possible, because those components are characterized by substantially different relaxation parameters. For this purpose, the obtained model curve (the solid curve in Fig. 4, a) was used as a reference, from which the ordinates of the experimental curve corresponding to the slow component were reckoned. The obtained function was also a straight line on the log scale, and its slope determined the characteristic time of the conductive component of heat transfer. The relaxation parameter of the process determined in such a way made it possible to obtain the curve shown in Fig. 4, b (the solid line). The same procedure applied to the difference between the model and general experimental curves was used to

obtain the model parameters of the fastest component. It is located between the model and experimental curves in the interval $0 < t < 0.4$ min. Its interpretation does not cause difficulties, if we take into account that the absorption and radiation effects are considered in the theory of radiation to be related with the surface [21].

In practice, however, the spectral intervals of the radiation and absorption spectra are determined by the temperature of a substance and its radiation emission coefficient. The latter, in turn, is determined by the type of a material and the properties of its surface [22]. Therefore, taking the Bouguer–Lambert law into account, the effective localization length of the absorbed (emitted) energy acquires finite values, which are determined, in the first approximation, by the product of the functional expressions for two laws. In this case, it is important that this and conductive components have opposite signs. The obtained result agrees with the conclusion of work [22] that if the absorption coefficients are large, the radiation emission effects can be observed only in a vicinity of the radiation region and are described by the diffusion equation for the radiation heat flux. Therefore, we may suppose that the corresponding time parameter $\tau_{\rm rad}$ has an effective value that is determined, as in the size effect, not only by the thermal conductivity coefficient, but also by the thickness of the layer, in which the energy absorption and/or radiation takes place. In Fig. 4, the right axes correspond to the phase difference change $\Delta\phi$, and the left ones to the mechanical stress calculated by normalizing $\Delta\phi$ by a value obtained from an additional measurement.

In Fig. 5, all three components of the heat transfer with parameters obtained from the decomposition of the first section of the general characteristic are compared. When superposing the curves, their amplitudes were changed by the difference between the ordinates of the initial and steady states of the model dependences (Fig. 4). The fact that the model curves have finite values at the initial time moment is not a paradox, because the balance of amplitudes with different signs provides a zero signal at the initial time moment. However, the balance of signed stress values is maintained throughout the relaxation period.

Figure 6 demonstrates the coordinate dependences of the total stress for three time values within the interval, during which the radiation component saturates. From the previous analysis, it follows that this component and the conductive one have different signs. This fact brings us to the conclusion that the radiation-induced stress is localized in the near-surface region of the specimen. There is no doubt that the ratio between the relaxation parameters of the heat transfer components will be strongly different in the coordinate representation. The determination of those parameters for various components is a matter of separate interest.

4. Conclusions

The kinetics of thermoelasticity induced by a radiation field in a flint glass specimen is studied in two regimes, cooling and heating. The method of modulation polarimetry is applied to register the mechanical stresses arising at a temperature difference of a few degrees across the specimen. The mechanical stress magnitude is found to be a linear function of the optical anisotropy value. Its kinetics measured at different points has a complicated character, which varies along the heat flux. Small temperature drops across the specimen, which were used in this work, enabled the general stress kinetics to be approximated as a sum of exponential dependences. Additional measurements showed their relation to the radiative, conductive, and convective components of heat transfer, which participate in the temperature field formations. By analyzing one of the dependences, the characteristic parameters (the amplitude and the relaxation time) are calculated for all three heat transfer mechanisms.

We would like to note that the combined radiation and convection cooling was considered in work [23]. The numerical solution of the corresponding nonlinear problem was presented there in a dimensionless graphical form for a wide range of parameters of the problem. The results obtained in the cited work are in a good qualitative agreement with ours. This cannot be said about work [12], where the effect of the thermal radiation cooling is very small, as a rule, in comparison with the convective cooling.

1. A.D. Kovalenko. *Fundamentals of Thermoelasticity* (Naukova Dumka, 1970) (in Russian).
2. W. Nowacki, Dynamiczne zagadnienia termosprezystosci (Panstwowe Wydawnictwo Naukowe, 1966).
3. K.L. Muratikov. Generation theory of mechanical vibrations by laser radiation in solids with internal stresses on the basis of thermoelastic effect. *Zh. Tekhn. Fiz.* **69**, No. 7, 59 (1999).

4. M.M. Frocht. *Photoelasticity* (Wiley, 1949).
5. T.S. Narasimhamurty. *Photoelastic and Electro-Optic Properties of Crystals* (Plenum Press, 1981).
6. A.Ya. Aleksandrov, M.Kh. Akhmetzyanov. *Polarization Optical Methods of Mechanics of Deformable Solids* (Nauka, 1973) (in Russian).
7. L.I. Berezhinsky, I.L. Berezhinsky, O.N. Grigorev, B.K. Serdega, V.A. Ukhimchuk. Investigation of residual stresses on the boundary of SiC/SiC+20% TiB_2 composite materials joining by optic modulation–polarization method. *J. Eur. Cer. Soc.* **27**, 2513 (2007).
8. M. Cardona. *Modulation Spectroscopy* (Academic Press, 1969).
9. I.E. Matyash, I.A. Minailova, O.N. Mishchuk, B.K. Serdega. Modulation polarimetry of thermoelasticity induced by thermal radiation in glass. *Fiz. Tverd. Tela* **56**, 1439 (2014) (in Russian).
10. O.R. Hachkevych, T.L. Kurnyts'kyi, R.F. Terlets'kyi, Mechanical-thermodiffusion processes in a semitransparent solid layer under the action of thermal infrared radiation. J. Math. Sci. **104**, 1542 (2001).
11. V.I. Pipa, A.I. Liptuga, Parameter analysis and optimization for the radiative cooling effect due to negative luminescence. *J. Appl. Phys.* **92**, 5053 (2002).
12. Y.B. Yi, A. Bendawi, Effect of convective cooling on frictionally excited thermoelastic instability. *Wear* **296**, 583 (2012).
13. Z. Wei, K.-M. Lee, S.W. Tchikanda, Z. Zhou, S.-P. Hong. Free surface flow in high speed fiber drawing with large-diameter preforms. *J. Heat Transf.* **126**, 635 (2004).
14. J. Norbeck, R. Horne. Injection-triggered seismicity: An investigation of porothermoelastic effects using a rate-and-state earthquake model. In *Proceedings of the 40th Workshop on Geothermal Reservoir Engineering* (Stanford, California, 2015), p. 524.
15. N. Fernandez, W. Wang, K. Alvine, S. Katipamula, *Energy Savings Potential of Radiative Cooling Technologies* (Pacific Northwest National Laboratory, 2015).
16. S. Ito, N. Miura. Studies of radiative cooling systems for storing thermal energy. *J. Sol. Ener. Eng.* **111**, 251 (1989).
17. J. Cui, Y. Wu, J. Muehlbauer, Y. Hwang, R. Radermacher, Demonstration of high efficiency elastocaloric cooling with large ΔT using NiTi wires. *Appl. Phys. Lett.* **101**, 073904 (2012).
18. S. Qian, J. Ling, Y. Hwang, R. Radermacher, I. Takeuchi. Thermodynamics cycle analysis and numerical modeling of thermoelastic cooling systems. *Int. J. Refrig.* **56**, 65 (2015).
19. A. Gerrard, J.M. Burch. *Introduction to Matrix Methods in Optics* (Dover, 1975).
20. E.G. Coker, L.N.G. Filon. *A Treatise on Photo-Elastisity* (Cambridge Univ. Press, 1931).
21. R. Siegel, J. Howell. *Thermal Radiation Heat Transfer* (Taylor and Francis, 2002).
22. M.F. Modest. *Radiative Heat Transfer* (Academic Press, 2003).
23. M.A. Yaghoubi, R. Manvi. Thermal stresses in transient cooling of a heat generating sphere. *Nucl. Eng. Des.* **33**, 381 (1975).

Received 20.11.17.
Translated from Ukrainian by O.I. Voitenko

І.Є. Матяш, І.А. Мінайлова,
О.М. Міщук, Б.К. Сердега

КОМПОНЕНТНИЙ АНАЛІЗ ТЕРМОПРУЖНОСТІ, ІНДУКОВАНОЇ РАДІАЦІЙНИМ ВИПРОМІНЮВАННЯМ, В ПРЕДСТАВЛЕННІ МОДУЛЯЦІЙНОЇ ПОЛЯРИМЕТРІЇ

Р е з ю м е

Радіаційне поле від зовнішнього або внутрішнього випромінювання створює в зразку зі скла неоднорідний градієнт температури. В цьому випадку виникає потік тепла у зразку, який генерує механічні напруження і, як наслідок, оптичну анізотропію у вигляді подвійного променезаломлення. Його величина виміряна оптико-поляризаційним методом у вигляді різниці фаз між ортогональними компонентами лінійно поляризованого зондуючого випромінювання. Виявна здатність методу підвищена модуляцією поляризації випромінювання, що забезпечує достовірну реєстрацію напружень у зразку при перепаді температури на рівні десятої градуса. Виявлена складна за формою і неоднозначна за знаком кінетика напруження в точці спостереження протягом часу встановлення. Її моделювання експонентними функціями дозволило виконати розкладання результату вимірювання на компоненти, пов'язані з радіаційним, кондуктивним і конвективним механізмами теплопередачі, а також визначити параметри їх релаксації. Результати вимірювань можуть мати практичне застосування у визначенні таких технічно важливих характеристик матеріалів, як коефіцієнти температуропровідності і теплопередачі.